EPSC Abstracts
Vol. 14, EPSC2020-75, 2020, updated on 08 Dec 2022
https://doi.org/10.5194/epsc2020-75
Europlanet Science Congress 2020

On the Methylacetylene Abundance and Nitrogen Isotope Ratio on Pluto

Vladimir Krasnopolsky
Moscow Institute of Physics and Technology, College Park, United States of America (vlad.krasn@verizon.net)

Intoduction. The recent progress in the studies of Pluto is related to the New Horizons flyby, and the solar and stellar occultations at 52-187 nm revealed vertical profiles of N_2, CH_4, C_2H_2, C_2H_4, and C_2H_6 (Gladstone et al. 2016, Young et al. 2018, Kammer et al. 2020). The ALMA submillimeter spectroscopy (Lellouch et al. 2017) gave a CO profile, abundance of $HC^{14}N$, and restrictive upper limits to $HC^{15}N$ and HC_3N. The photochemical model of Pluto's atmosphere and ionosphere (Krasnopolsky 2020) reproduces fairly well these data. Recently methylacetylene and atomic hydrogen were detected using UV spectroscopy from New Horizons (Steffl et al. 2020).

Metylacetylene C_3H_4abundance of 5×10^{15} cm^{-2} observed from New Horizons is close to 7.7×10^{15} cm^{-2} in our early model (Krasnopolsky and Cruikshank 1999) but exceeds 9×10^{14} cm^{-2} in Krasnopolsky (2020). To bring the model into agreement with the observation, rate coefficients of the three key reactions of C_3H_4 production and removal are changed to the values calculated by Vuitton et al. (2019). The calculated C_3H_4 abundance is 4.3×10^{15} cm^{-2} (Figure 1).

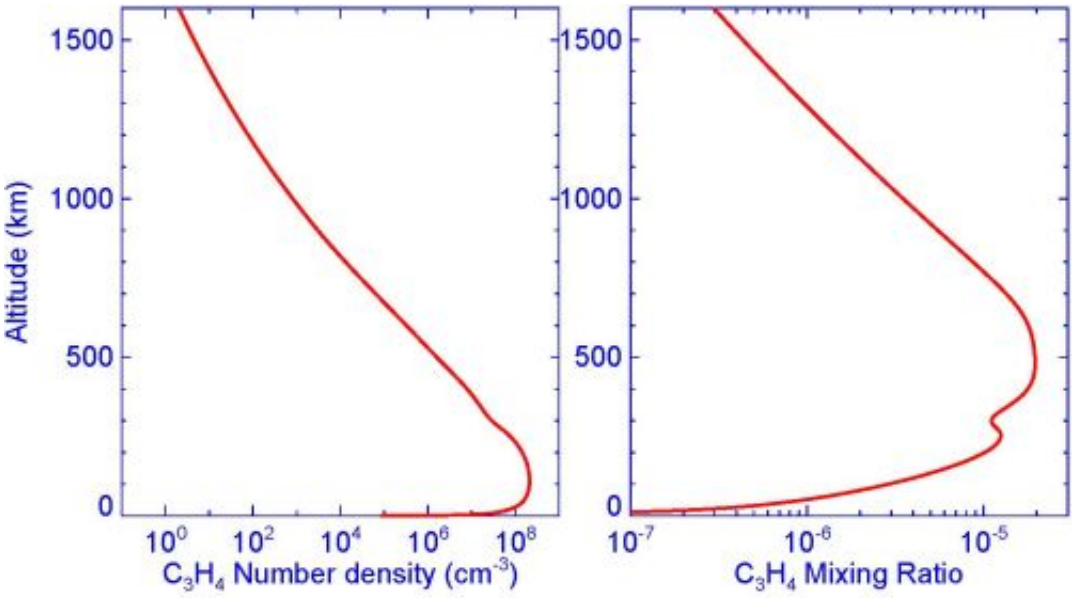

Fig. 1. Vertical profiles of C3H4 number density and mixing ratio on Pluto

Table 1. Some column abundances, production and loss rates, escape/precipitation flows, and chemical lifetimes

Species	C_3H_4	H	H_2	C_2H_2	C_2H_4	C_2H_6	C_3H_8	C_4H_2	HCN	HC_3N
Column abundance (cm^{-2})*	8.9+14	7.0+14	3.3+16	2.4+16	5.5+15	7.7+16	9.0+14	3.0+14	1.7+14	3.9+13
Column abundance (cm^{-2})	4.3+15	5.3+14	4.3+16	2.3+16	5.7+15	7.4+16	1.2+15	2.3+14	1.7+14	2.3+13
Production (cm^{-2} s^{-1})	6.76+7	8.57+8	6.23+8	2.06+8	1.84+8	8.24+7	2.26+6	6.83+7	8.84+7	1.36+7
Loss (cm^{-2} s^{-1})	5.31+7	3.66+8	2.72+6	8.49+7	1.84+8	4.32+7	4.08+5	5.06+7	6.36+7	6.82+5
Flow (g cm^{-2} Byr^{-1})	-30.3	25.8	65.0	-166	-0.4	-62	-4.3	-46	-35	-35
Lifetime (yr)	2.6	0.03	2.6	4.5	1.6	36	21	0.16	0.12	0.08

Production and loss refer to photochemical reactions; positive flows are escape, negative flows are condensations; production, loss, and flow are reduced to the surface; 4.3+15 = 4.3×10^{15} cm^{-2}.

* This row refers to Krasnopolsky (2020).

Main reactions of production and loss of C_3H_4 are shown in Figure 2. Column abundances of some species in the model and its previous version are shown in Table 1 along with production and loss rates, escape and precipitation flows, and chemical lifetimes. The HC_3N abundance of 2.3×10^{13} cm^{-2} in the model is close to the upper limit of 2×10^{13} cm^{-2} (Lellouch et al. 2017). The change in the model increases H_2 and C_3H_8 by factors of 1.3 and reduces H and C_4H_2 by factors of 1.3, while the other species remain almost unchanged relative Krasnopolsky (2020).

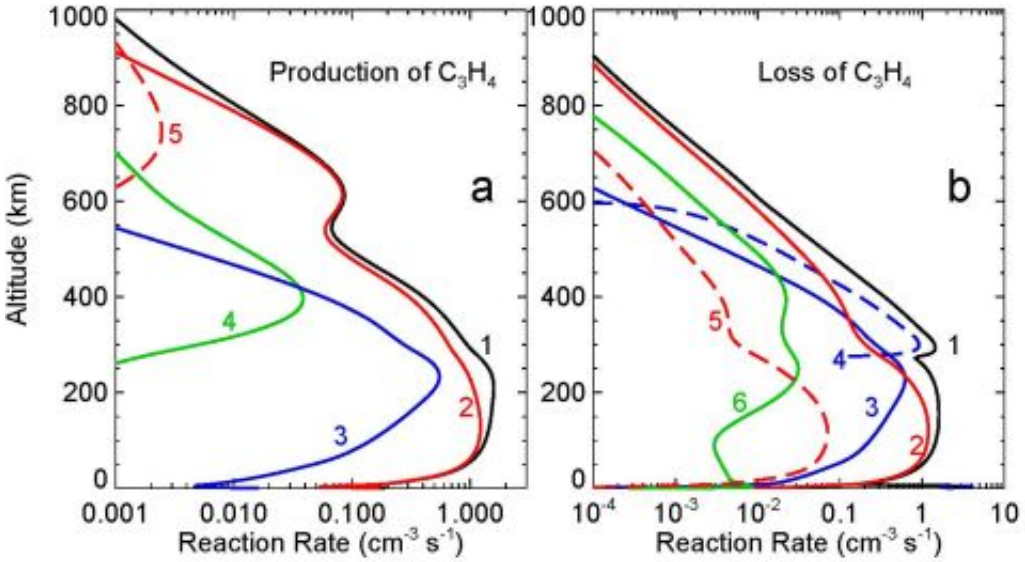

Fig. 2. Main reactions of production and loss of C3H4. Production (a): 1 - total, 2 -C3H3 + H (+ M) -> C3H4 (+ M), 3 - C3H5 + H -> C3H4 + H2, 4 - C2H4 + CH -> C3H4 + H, 5 - $C4H5^+$ + e -> C3H4 + CH. Loss (b): 1 - total, 2 - photolysis, 3 - C3H4 + H (+M) -> C3H5 (+ M), 4 - condensation, 5 - C3H4 + C2H->C3H3 +C2H2, 6 - C3H4 +CN->C3H3 +HCN

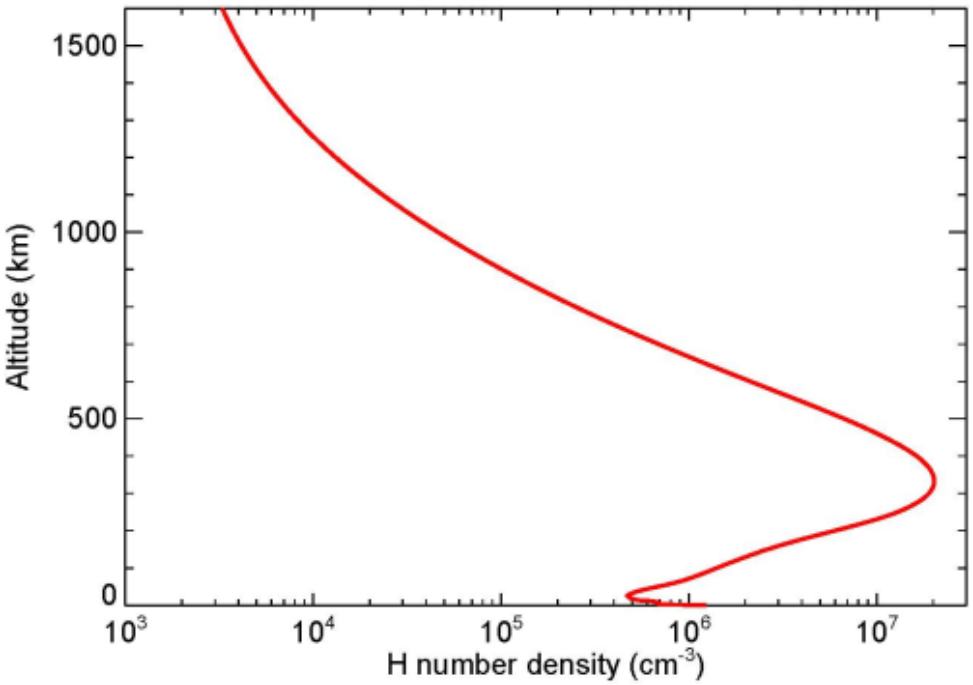

Fig. 3. Calculated profile of atomic hydrogen

Atomic hydrogen abundance of $(7.7\pm1.7)\times10^{13}$ cm^{-2} at τ=1 (490 km) was measured (Steffl et al. 2020) using the observed Lyman-beta emission. This value is 6.9×10^{13} cm^{-2} in our model (Fig.3) and 7.3×10^{13} cm^{-2} in the previous version (Krasnopolsky 2020).

Reflectivity of 0.17 at 140-185 nm (Steffl et al. 2020) agrees with the HST value of 0.14 at 180-190 nm (Krasnopolsky 2001).

Nitrogen isotope ratio. The observed lower limit $HC^{14}N/HC^{15}N$ > 125 on Pluto (Lellouch et a. 2017) agrees with $^{14}N/^{15}N$ in the planets, asteroids, comets, and the solar wind. However, it looks puzzling compared to $HC^{14}N/HC^{15}N$ = 60 on Titan that is perfectly explained by predissociation of N_2 at 80-100 nm (Liang et al. 2007, Krasnopolsky 2016). Both Pluto and Titan have nitrogen-methane atmospheres with significant similarity in photochemistry.

Major reactions of production and loss of HCN on Pluto are given in Table 2. Our analysis confirms predissociation of N_2 at 80-100 nm as the major process of nitrogen isotope fractionation on Pluto. Kinetic isotope effect induced by difference of reduced mass of the reactants is very small, for example, k_{14}/k_{15} = 1.006 for CH + HCN -> CHCN + H. Our calculation gives negligible photo-induced isotope fractionation for HCN. Isotope fractionation in condensation of ammonia is calculated at 1.04 for Pluto's conditions using measurements by King et al. (1989). This value is adopted for HCN on Pluto.

Table 2. Major reactions of production and loss of HCN on Pluto

Production			Loss		
#	Reaction	Column rate	#	Reaction	Column rate
1	$H_2CN + H \rightarrow HCN + H_2$	3.97+7[a]	1	$CH + HCN \rightarrow CHCN + H$	4.46+7
2	$CN + C_2H_4 \rightarrow HCN + C_2H_3$	1.51+7	2	ion reactions	1.65+7
3	$HCNH^+ + \ldots \rightarrow HCN + \ldots$	1.89+7	3	photolysis	2.36+6
4	other ion reactions	9.03+6	4	condensation	2.48+7
5	Total[b]	8.84+7	5	Total[b]	8.84+7

[a] Scaled to the surface, 3.97+7 = 3.97×10^7 cm^{-2} s^{-1}.
[b] Including reactions that are not shown here.

The observed twofold difference on Pluto is partially caused by diffusive depletion of the heavy isotope in HCN and in predissociation of N_2. On Pluto, mean altitudes of HCN and predissociation of N_2 are 500 and 860 km, well above the homopause at 96 km. On Titan, the observations of $HC^{14}N/HC^{15}N$ refer to 90-460 km (Vinatier et al. 2007), predissociation happens near 985 km, both below the homopause at 1000 km, and diffusive depletion does not occur. Therefore the observed limit corresponds to $^{14}N/^{15}N > 253$ for N_2 in the lower atmosphere and $^{14}N/^{15}N > 228$ in the upper layers of the N_2 ice. These limits reflect the conditions on Pluto in the last two million years. The current loss of N_2 is 37.5 g cm^{-2} Byr^{-1} primarily to photodestruction. The calculated isotope fractionation factor of 1.96 accounts for formation and condensation of nitriles, diffusive separation, and fractionation in thermal escape. Variations of $^{14}N/^{15}N$ in the N_2 ice are relevant to evolution of the solar EUV, mixing processes in the N_2 ice, and possible periods of hydrodynamic escape that are poorly known and not considered here.

References

Gladstone, G.R., et al., 2016. Science 351 (6279), aad8866.

Kammer, J.A., et al., 2020. Astron. J. 159, 26 (9pp).

King, T.V., et al., 1989. Z. Naturforsch. 44a, 359-370.

Krasnopolsky, V.A., 2001. Icarus 153, 277-284.

Krasnopolsky, V.A., 2016. Planet. Space Sci. 134, 61-63.

Krasnopolsky, V.A., 2020. Icarus 335, 113374.

Krasnopolsky, V.A., Cruikshank, D.P., 1999. J. Geophys. Res. 104, 21979–21996.

Lellouch, E., et al., 2017. Icarus 286, 289-307.

Liang, M.C., et al., 2007. Astrophys. J. Lett. 664, L115-L118.

Steffl, A.J., et al., 2020. Astron. J. 159, 274 (12pp).

Vinatier, S., Bezard, B., Nixon, C.A., 2007. Icarus 191, 712-721.

Vuitton, V., Yelle, R.V., Klippenstein, S.J., H□rst, S.M., Lavvas, P., 2019. Icarus 324, 120-197 (supplementary material).

Young, L.A., et al., 2018. Icarus 300, 174-199.